26th INTERNATIONAL CONGRESS ON SOUND AND VIBRATION
7-11 July 2019, Montreal

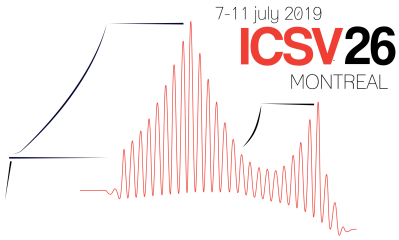

ACTIVE STRUCTURAL ACOUSTIC CONTROL OF A FLAT PLATE USING AN EXPERIMENTALLY IDENTIFIED RADIATION RESISTANCE MATRIX

Joseph Milton, Jordan Cheer *and* Steve Daley
Institute of Sound and Vibration Research (ISVR), University of Southampton, Southampton, UK
email: j.milton@soton.ac.uk

Active Structural Acoustic Control (ASAC) is a widely used active noise control technique, which provides global control of structurally radiated noise by controlling structural vibrations. Many current ASAC systems rely upon the availability of an accurate, real-time measure of the radiated sound field. This often requires positioning of acoustic error sensors in the radiated sound field, which for many practical setups may not always be possible. Previous research has investigated the implementation of ASAC using structural measurements that can be related to the radiated noise. One such method employs the use of the radiation resistance matrix to estimate the radiated sound power from structural measurements. However, estimation of the radiation resistance matrix has generally relied upon precise modelling of the radiating structure which, for practical structures, can lead to limitations in the accuracy of the estimate. To overcome this problem, this paper presents an ASAC system that utilises an experimentally identified radiation resistance matrix. It is shown via real-time implementation of the proposed strategy for a flat plate, that the proposed ASAC system is effective at controlling structurally radiated noise and out performs an Active Vibration Control (AVC) system using identical hardware. At the first three radiating modes, the proposed method achieves 9, 9 and 23 dB more attenuation in the radiated sound power than AVC.
Keywords: Active Structural Acoustic Control (ASAC), Radiation Resistance Matrix

1. Introduction

Structurally radiated sound can be directly related to the motion of the radiating structure and thus, by controlling the radiating structure itself, control of the radiated sound field can be achieved. Active Structural Acoustic Control (ASAC) is a control strategy which, in its most basic form, aims to reduce structurally radiated noise by interfering with the vibrating structure using secondary structural sources which are driven to minimise the sound pressure measured at error microphones located in the radiated sound field [1, 2]. One of the main limitations of such ASAC strategies is that it is often not practical to position error microphones in the radiated sound field. This has led to a number of different ASAC strategies being developed which aim to minimise quantities that, not only reduce the radiated sound field, but do not interfere with the operation of the radiating structure itself. These approaches require only structural error sensors and a model or operating function that estimates the sound radiated from the structure [3, 4, 5, 6, 7].

A number of these approaches utilise an estimate of the radiated sound power as the cost function, as this provides a single global quantity for the ASAC system to minimise. Recently, a method for estimating radiated sound power using only structural responses and an experimentally identified

radiation resistance matrix has been proposed [8]. This approach identifies the radiation resistance matrix of a structure using the transfer responses between a distribution of structural actuators and a measure of the structural and acoustic responses.

In this paper, the performance of a tonal ASAC strategy, which utilises the experimentally identified radiation resistance matrix, is investigated. Utilising the same actuator distribution that is used to identify the radiation resistance matrix, the proposed ASAC strategy is implemented on an acoustically excited plate and the sound power attenuation performance of the strategy is compared to that of an Active Vibration Control (AVC) system, under identical conditions.

The structure of this paper is as follows; Section 2 summaries the method for experimental identification of the radiation resistance matrix. Section 3 defines the AVC and proposed ASAC systems. In Section 4, the performance of the proposed ASAC strategy is compared to that of AVC for the tonal control of an acoustically excited plate. Finally, Section 5 draws conclusions based on the results of the study.

2. Experimental identification of the radiation resistance matrix

In this section, the experimentally identified radiation resistance matrix is formulated and the identification procedure is described as previously presented in [8]. Typically, radiated sound power is calculated using a number of particle velocity and acoustic pressure measurements, recorded over a virtual surface enclosing the radiating structure. The radiated sound power can thus be calculated in practice as

$$W = \left(\frac{A}{2}\right) \mathbb{R}\mathrm{e}\{\mathbf{p}^H \mathbf{u}\}, \tag{1}$$

where $\mathbf{p}$ is the vector of acoustic pressure measurements, $\mathbf{u}$ is the vector of particle velocity measurements and A is the area over which the particle velocities and acoustic pressures are measured divided by the number of measurement positions. These acoustic pressures and particle velocities can be expressed in terms of the structural response as

$$\mathbf{p} = \widetilde{\mathbf{H}}_p \mathbf{q}, \quad \text{and} \quad \mathbf{u} = \widetilde{\mathbf{H}}_u \mathbf{q}, \tag{2}$$

where $\mathbf{q}$ is the vector of structural responses measured on the surface of the structure, which could be represented by accelerations, velocities or displacements, and $\widetilde{\mathbf{H}}_p$ and $\widetilde{\mathbf{H}}_u$ are the transfer response matrices between the structural response and the acoustic pressures and particle velocities respectively. By substituting Eq. 2 into Eq. 1 for the vectors of acoustic pressure and particle velocity, the radiated sound power can be written in terms of the structural responses as,

$$W = \left(\frac{A}{2}\right) \mathbb{R}\mathrm{e}\{\mathbf{q}^H \widetilde{\mathbf{H}}_p^H \widetilde{\mathbf{H}}_u \mathbf{q}\}. \tag{3}$$

Expanding this in terms of its real and imaginary parts allows a simplification that gives

$$W = \left(\frac{A}{4}\right) \mathbf{q}^H [\Xi^H + \Xi] \mathbf{q} = \mathbf{q}^H \mathbf{R} \mathbf{q}, \tag{4}$$

where $\Xi = \widetilde{\mathbf{H}}_p^H \widetilde{\mathbf{H}}_u$ and the experimentally identified radiation resistance matrix is defined as $\mathbf{R} = (A/2)\, \mathbb{R}\mathrm{e}[\widetilde{\mathbf{H}}_p^H \widetilde{\mathbf{H}}_u]$. This appears to provide a direct means of calculating the radiation resistance matrix, however, it is not possible to measure the matrices $\widetilde{\mathbf{H}}_p$ and $\widetilde{\mathbf{H}}_u$ directly, as each of the structural responses cannot be independently driven and are only controllable via a fully coupled transfer response matrix [6]. It is possible to estimate these matrices, however, via the solution of an inverse problem [6, 8, 9].

This inverse problem can be formulated by first expressing the vector of structural responses in terms of a distribution of structural forces, $\mathbf{f}$, and a transfer response matrix as

$$\mathbf{q} = \mathbf{H}_s\mathbf{f}, \tag{5}$$

where $\mathbf{H}_s$ is the matrix of transfer responses between the distribution of independent forces and the structural response, which can be measured directly. The vectors of acoustic pressures and particle velocities can then be defined by substituting Eq. 5 into Eq. 2 to give

$$\mathbf{p} = \widetilde{\mathbf{H}}_p\mathbf{H}_s\mathbf{f} \quad \text{and} \quad \mathbf{u} = \widetilde{\mathbf{H}}_u\mathbf{H}_s\mathbf{f}, \tag{6}$$

where

$$\mathbf{H}_p = \widetilde{\mathbf{H}}_p\mathbf{H}_s \quad \text{and} \quad \mathbf{H}_u = \widetilde{\mathbf{H}}_u\mathbf{H}_s, \tag{7}$$

which represent the measurable matrices of transfer responses between the distribution of forces and the acoustic pressures and particle velocities respectively. Provided that the number of structural measurements is equal to the number of forces, so that $\mathbf{H}_s$ is a square matrix, Eq. 7 can be rearranged to calculate the matrices $\widetilde{\mathbf{H}}_p$ and $\widetilde{\mathbf{H}}_u$ by solving the inverse problems,

$$\widetilde{\mathbf{H}}_p = \mathbf{H}_p\mathbf{H}_s^{-1} \quad \text{and} \quad \widetilde{\mathbf{H}}_u = \mathbf{H}_u\mathbf{H}_s^{-1}. \tag{8}$$

If the structural response matrix, $\mathbf{H}_s$, is not square, the solution to the inverse problem must be calculated via the pseudo-inverse [8].

3. Active structural control strategies

In this section two active structural control strategies are formulated, the first, AVC, aims to minimise the level of vibration measured on the surface of a structure directly. The second strategy, ASAC, aims to minimise an estimate of the radiated sound power obtained using measurements taken on the surface of the structure along with the radiation resistance matrix.

3.1 Active vibration control

AVC in this case aims to minimise the sum of the squared signals measured at L structural error sensors, which can be defined at a single frequency by the cost function

$$J_s = \mathbf{e}^H\mathbf{e}, \tag{9}$$

where $\mathbf{e}$ is the vector of L error signals, in the steady state, measured on the surface of the panel. The vector of error signals, $\mathbf{e}$, can be defined by the linear superposition of the primary disturbance measured at each sensor position, $\mathbf{d}$, and the contribution due to the controller, $\mathbf{Gu}$,

$$\mathbf{e} = \mathbf{d} + \mathbf{Gu}, \tag{10}$$

where $\mathbf{d}$ is the vector of L primary disturbances, $\mathbf{u}$ is the vector of M control signals and $\mathbf{G}$ is the $(L \times M)$ matrix of transfer responses between the structural control actuators and the error signals measured at each sensor location. Substituting Eq. 10 into Eq. 9 gives the cost function as

$$J_s = \mathbf{u}^H\mathbf{G}^H\mathbf{Gu} + \mathbf{d}^H\mathbf{Gu} + \mathbf{u}^H\mathbf{G}^H\mathbf{d} + \mathbf{d}^H\mathbf{d}. \tag{11}$$

If the matrix $\mathbf{G}^H\mathbf{G}$ is assumed to be positive definite, which is generally the case [10], then the control signals that minimise the cost function, J_s, are generated by setting the derivative of eqn.11 with respect to the real and imaginary parts of $\mathbf{u}$ to zero. The optimal vector of control signals is then

$$\mathbf{u}_{opt} = -[\mathbf{G}^H\mathbf{G}]^{-1}\mathbf{G}^H\mathbf{d}. \tag{12}$$

If $L = M$, which is the case for the controllers in this paper, then the optimal vector of control signals becomes

$$\mathbf{u}_{opt} = -\mathbf{G}^{-1}\mathbf{d}. \tag{13}$$

For practical applications, the disturbance signals are not known in advance and therefore, to minimise the sum of squared error signals in real-time, an algorithm that is able to iteratively adjust the input to the control actuators, $\mathbf{u}$, is needed. In this case, the method of steepest decent has been used to manipulate the measured signals and drive the control actuators to minimise the sum of the squared error signals. The update algorithm used by this AVC system is

$$\mathbf{u}(n+1) = \gamma\,\mathbf{u}(n) - \alpha\,\mathbf{G}^{H}\,\mathbf{e}(n), \tag{14}$$

where n represents the current iteration step of the algorithm, γ is the leakage factor and α is the convergence gain of the controller.

3.2 Active structural acoustic control using the radiation resistance matrix

The ASAC strategy presented in this paper utilises the experimentally identified radiation resistance matrix along with structurally measured error signals in order to minimise a cost function that reduces structurally radiated sound power. Using the radiation resistance matrix along with the structural response as per Eq. 4, the ASAC cost function to minimise is defined as

$$J_W = \mathbf{e}^{H}\mathbf{R}\mathbf{e}, \tag{15}$$

where $\mathbf{e}$ is the vector of structurally measured error sensor signals. Whilst the radiation resistance matrix, $\mathbf{R}$, can be used to estimate the radiated sound power from an excited structure, as in Eq. 4, it is not guaranteed to be positive definite. Therefore, the cost function defined in Eq. 15 is not guaranteed to have a global minimum. For this reason, further steps must be taken in order to enforce positive definiteness on the radiation resistance matrix.

This problem has been approached previously for use in a broadband control system by [6], by calculating a linear time invariant (LTI) model of a power transfer matrix via a non-convex optimisation procedure, followed by further optimisation to ensure positive definiteness. However, for tonal control this method is overly complex and is likely to limit the performance and stability of the control system when excited off-resonance, due to limitations in the accuracy of the LTI model. For the tonal radiation problem considered here, these limitations can be overcome via direct calculation of the nearest positive semidefinite matrix approximation of the radiation resistance matrix from the frequency response data. This approximant can then be used in place of $\mathbf{R}$ in Eq. 15, so that the cost function has a single global minimum.

3.2.1 Positive semidefinite approximation of the radiation resistance matrix

The nearest positive semidefinite matrix that approximates the radiation resistance matrix can be found using one of two methods, which use either the 2-norm or Frobenius norm method [11]. The nearest positive semidefinite matrix is given according to the Frobenius norm by minimising

$$||\mathbf{R} - \widehat{\mathbf{R}}||_F^2, \tag{16}$$

where $\widehat{\mathbf{R}}$ is the positive semi-definite approximant of the radiation resistance matrix, $\mathbf{R}$. The solution in this case is [11]

$$\widehat{\mathbf{R}} = \frac{\mathbf{B} + \mathbf{H}}{2}, \tag{17}$$

where the symmetric part of $\mathbf{R}$ is given by $\mathbf{B} = (\mathbf{R} + \mathbf{R}^{H})/2$ and the positive Hermitian matrix, $\mathbf{H}$, is given by the polar decomposition of $\mathbf{B}$, which is given as $\mathbf{B} = \mathbf{U}\mathbf{H}$, where $\mathbf{U}^{T}\mathbf{U} = 1$ and

$\mathbf{H}^T\mathbf{H} \geq 0$. Alternatively, the symmetric positive semidefinite radiation resistance matrix, $\widehat{\mathbf{R}}$, can also be calculated from the eigenvalue decomposition of $\mathbf{B}$, which is given as [11]

$$\mathbf{B} = \mathbf{Z}\mathbf{\Lambda}\mathbf{Z}^{-1} \tag{18}$$

where $\mathbf{Z}$ is the matrix of eigenvectors and $\mathbf{\Lambda}$ is the diagonal matrix of eigenvalues, λ_i. The positive semidefinite approximant of the radiation resistance matrix, $\mathbf{R}$, is then

$$\widehat{\mathbf{R}} = \mathbf{Z}\mathbf{Y}\mathbf{Z}^{-1} \tag{19}$$

where $\mathbf{Y}$ is the diagonal matrix formed from the eigenvalues of $\mathbf{\Lambda}$ according to

$$y_i = \lambda_i, \quad \text{if } \lambda_i \geq 0 \quad \text{and} \quad y_i = 0, \quad \text{if } \lambda_i < 0. \tag{20}$$

That is, $\mathbf{Y}$ contains the positive eigenvalues of $\widehat{\mathbf{R}}$ and the negative eigenvalues are set to zero. Substituting the positive semi-definite radiation resistance matrix approximant into Eq. 15, the ASAC cost function that has a single global minimum is defined as

$$J_W = \mathbf{e}^H\widehat{\mathbf{R}}\mathbf{e}. \tag{21}$$

Substituting Eq. 10 for the structural error signals into Eq. 21 and expanding, the cost function becomes

$$J_W = (\mathbf{d} + \mathbf{G}\mathbf{u})\widehat{\mathbf{R}}(\mathbf{d} + \mathbf{G}\mathbf{u}) = \mathbf{u}^H\mathbf{G}^H\widehat{\mathbf{R}}\mathbf{G}\mathbf{u} + \mathbf{d}^H\widehat{\mathbf{R}}\mathbf{G}\mathbf{u} + \mathbf{u}^H\mathbf{G}^H\widehat{\mathbf{R}}\mathbf{d} + \mathbf{d}^H\widehat{\mathbf{R}}\mathbf{d}. \tag{22}$$

Again, the vector of optimal control signals, $\mathbf{u}_{opt}$, is obtained by setting the derivative of Eq. 22, with respect to the real and imaginary parts of $\mathbf{u}$ to zero, giving the vector of optimal control signals as

$$\mathbf{u}_{opt} = -\left[\mathbf{G}^H\widehat{\mathbf{R}}\mathbf{G}\right]^{-1}\mathbf{G}^H\widehat{\mathbf{R}}\mathbf{d}. \tag{23}$$

As in Section 3.1, in practice, since the disturbance signals are not known in advance, an iterative algorithm is required to minimise the cost function. The method of steepest decent has been used to adapt the control signals towards the optimal solution that minimises the radiated sound power estimate, which gives the update equation as

$$\mathbf{u}(n+1) = \gamma\,\mathbf{u}(n) - \alpha\,\widehat{\mathbf{G}}^H\widehat{\mathbf{R}}\,\mathbf{e}(n). \tag{24}$$

4. Experimental investigation

In this section, the ASAC strategy has been implemented in real-time to control the sound radiated from a tonally excited plate. The performance of the proposed ASAC strategy has been compared, in terms of radiated sound power attenuation, to a standard centralised AVC system at three resonance frequencies.

4.1 System description

A flat aluminium plate has been used to assess the performance of the proposed ASAC strategy. The plate was mounted on a rigid enclosure and 12, approximately collocated, actuators and accelerometers were fixed to the surface. Figure 1 shows photographs of the plate with the actuator and accelerometer arrangement in place. To obtain the transfer responses required to generate the radiation resistance matrix for the plate, each actuator was independently driven with broadband noise. The structural response was measured using the array of accelerometers and the particle velocities and acoustic pressures were measured at approximately 0.1 m above each accelerometer position [8].

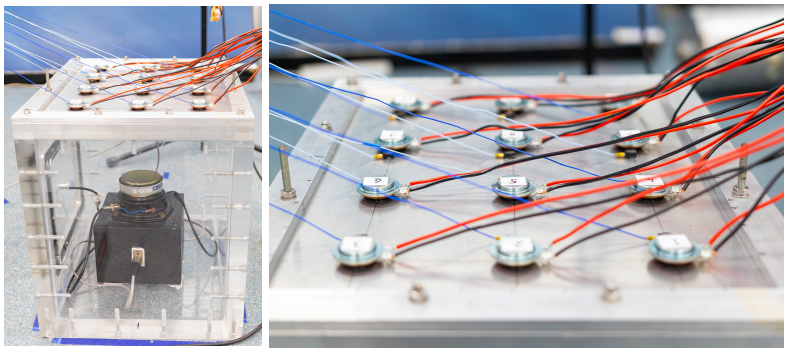

Figure 1: Photographs showing the plate mounted to a rigid enclosure which contains the primary disturbance, a volumetric loudspeaker. Fixed to the surface of the plate are 12 evenly space actuators, each approximately collocated with a measurement accelerometer.

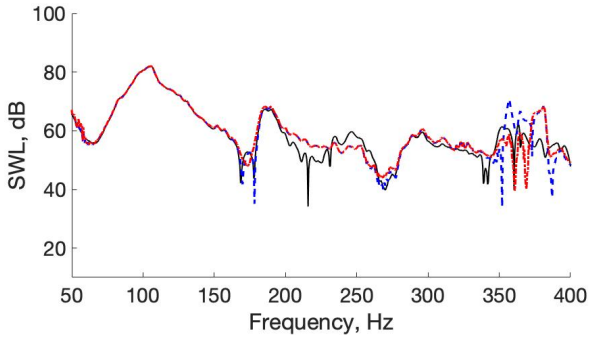

Figure 2: Sound power radiated from the plate shown in Fig. 1, measured directly (solid black line), estimated using the radiation resistance matrix (dashed blue line) and using the radiation resistance matrix approximant (dash-dotted red line).

The radiated sound power was estimated using both the radiation resistance matrix and the radiation resistance matrix approximant, these are shown in Fig. 2 plotted along with the directly measured sound power. Figure 2 shows that the sound power estimated using the radiation resistance matrix and the radiation resistance matrix approximant are approximately equivalent across the presented frequency range. Compared to the measured sound power, the estimated sound power is also accurate in level and resonance identification. Three resonance frequencies; 105, 186 and 297 Hz, have been selected to investigate the performance of the proposed tonal ASAC strategy. Fig. 3 shows the mode shapes of the plate that radiate at these frequencies.

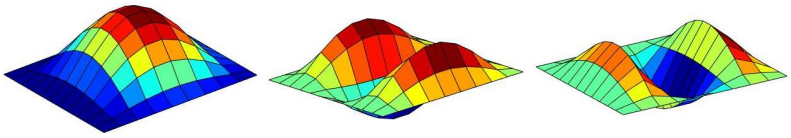

(a) 105 Hz - (1,1) (b) 186 Hz - (1,3) (c) 297 Hz - (3,1)

Figure 3: Mode shapes of the plate at the selected resonance frequencies.

4.2 Real-time validation of the proposed ASAC strategy

In this section, the results of the comparison between the AVC and proposed ASAC strategies are shown. To investigate the performance of each control strategy, the plate shown in Fig. 1 was excited acoustically at each of the selected resonance frequencies. The two control strategies were then implemented, minimising the cost functions defined in Section 3, using the same 4 by 3 array of

actuators and errors sensors that was used to identify the radiation resistance matrix in Section 2. The convergence gain and leakage factor for each update algorithm were set so that for each cost function, the initial convergence was as quick as possible whilst remaining stable.

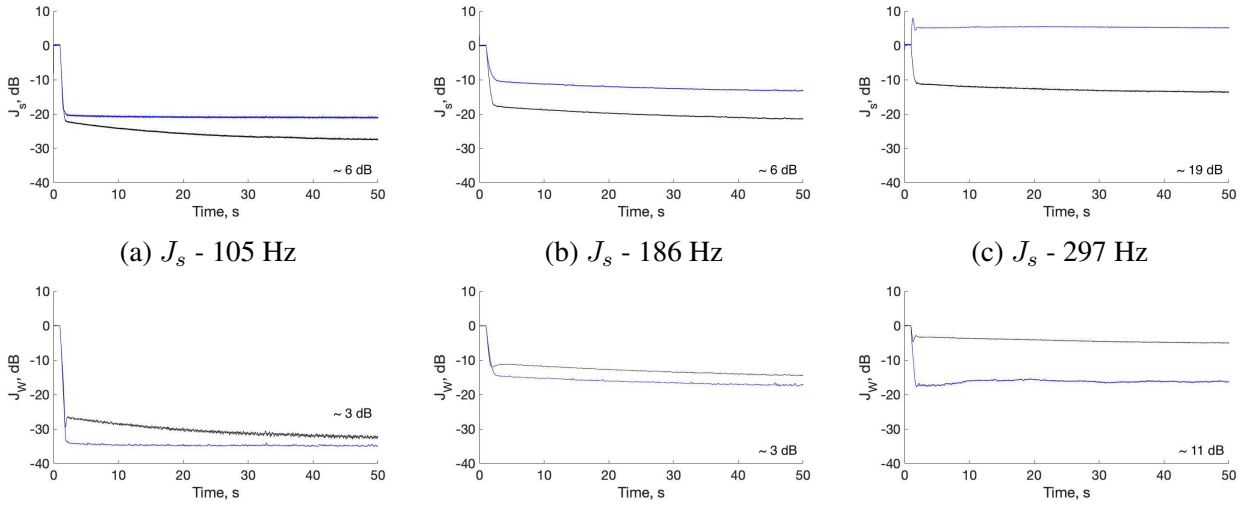

(a) J_s - 105 Hz (b) J_s - 186 Hz (c) J_s - 297 Hz

(d) J_W - 105 Hz (e) J_W - 186 Hz (f) J_W - 297 Hz

Figure 4: Attenuation of the structural cost function, J_s, and sound power cost function, J_W, when the plate is controlled tonally at 105, 186 and 297 Hz. In each plot the convergence of the AVC system is shown by the black line and the convergence of the proposed ASAC system is shown by the blue line.

Figure 4 shows the convergence of the cost functions J_s and J_W when the plate is excited and controlled tonally at each resonance. The difference between the converged AVC and ASAC cost functions is also shown in each plot. These results show that once both controllers have converged, AVC achieves approximately 6, 6 and 18 dB more attenuation in the structural vibration, at the three resonances, than ASAC, whilst the ASAC strategy is able to reduce the estimated sound power by approximately 3, 3 and 11 dB more than AVC.

Although the results presented in Fig. 4 have demonstrated that AVC and ASAC control the structural response and sound power radiation estimate more effectively respectively, it is important to validate the effect on the actual radiated sound power. To measure the actual radiated sound power, a number of acoustic pressure and particle velocity measurements were taken on a virtual surface in the radiated sound field above the plate, before and after each controller had converged. The radiated sound power was then calculated using Eq. 1 and the resulting increases in sound power attenuation provided by the ASC strategy are present in Table 1. In each case, ASAC achieves a significant performance advantage over AVC and thus validates the proposed sound power estimation method.

Table 1: Table showing the difference between the sound power attenuation achieved by ASAC and AVC, at each frequency.

Frequency Mode	$105\ Hz$ $(1,1)$	$186\ Hz$ $(1,3)$	$297\ Hz$ $(3,1)$
Performance benefit using ASAC	$9\ dB$	$9\ dB$	$23\ dB$

5. Conclusions

ASAC is an effective strategy for reducing the sound radiated by an excited structure. Although a variety of different ASAC strategies have been developed, few directly control the radiated sound power and many rely on error sensors located in the radiated sound field, which is often not practical.

In this paper, an ASAC strategy that utilises the radiation resistance matrix has been proposed. This strategy aims to minimise an estimate of the radiated sound power using only structurally located error sensors and control actuators.

The proposed ASAC strategy utilises the radiation resistance matrix to define a cost function that aims to estimate and minimise the radiated sound power. This strategy requires an initial calibration to identify the radiation resistance matrix for the structure. This is done by measuring the transfer response between a number of actuators on the surface of the structure and a number of structural and acoustic sensors. This same structural force - sensor arrangement can then be used as the actuation and sensing components for the control system which aims to minimise the structurally radiated sound power estimated using the radiation resistance matrix and the structural error sensors.

To provide an assessment of the performance of the proposed ASAC strategy, it has been used to control the sound radiation from a tonally excited plate at the first three radiating modes. These results were compared to those achieved by an AVC system that used an identical arrangement of sensors and actuators. It has been shown that at the three radiating modes ASAC is able to achieve an increased attenuation in the radiated sound power compared to AVC. It has also been shown that the difference between the performance of the AVC and ASAC systems increases as the order of the radiating modes increases. This is potentially as a result of the radiating mode shapes becoming more complex at higher frequencies and simply controlling the level of vibration across the plate becomes less effective than manipulating the shape of the radiating structure, this is demonstrated by the increase in vibration at 297 Hz when using ASAC.

Acknowledgements

This research was partially supported by an EPRSC iCASE studentship (Voucher number 15220040) and an EPSRC Prosperity Partnership (EP/S03661X/1).

References

1. Fuller, C., Elliott, S. and Nelson, P., *Active control of vibration*, Academic Press London (1996).
2. Fahy, F. and Gardonio, P., *Sound and structural vibration*, Academic Press Oxford (2007).
3. Baumann, W. T., Ho, F.-S. and Robertshaw, H. H. Active structural acoustic control of broadband disturbances, *The Journal of the Acoustical Society of America*, **92** (4), 1998 – 2005, (1992).
4. Cheer, J. and Daley, S. Active structural acoustic control using the remote sensor method, *Journal of Physics: Conference Series*, **744** (1), 012184, (2016).
5. Hendricks, D. R., Johnson, W. R., Sommerfeldt, S. D. and Blotter, J. D. Experimental active structural acoustic control of simply supported plates using a weighted sum of spatial gradients, *The Journal of the Acoustical Society of America*, **136** (5), 2598–2608, (2014).
6. Janda, O., Stein, G. L., Konigorski, U. and Heuss, O. Identification of power transfer matrices for active structural acoustic control, *20th International congress on sound and vibration*, ICSV20, (2013).
7. Elliott, S. and Johnson, M. E. Radiation modes and the active control of sound power, *Journal of the Acoustical Society of America*, **94** (4), 2194–2204, (1993).
8. Milton, J., Cheer, J. and Daley, S. An inverse method for the identification of the radiation resistance matrix from measurable acoustic and structural responses, *24th International congress on sound and vibration*, (2018).
9. Pintelon, R. and Schoukens, J., *System Identification: A Frequency Domain Approach*, John Wiley and Sons (2012).
10. Elliott, S. J., *Signal Processing for Active Control*, Academic Press London (2000).
11. Higham, N. J. Computing a nearest symmetric positive semidefinite matrix, *Linear algebra and it's applications*, **103** (103 - 118), (1988).